Parametric Booster Tankage Design Studies

WILLIAM H. MORITA*
North American Aviation, Inc., Downey, Calif.

These studies involve investigation of three structural materials: aluminum, steel, and tantanium alloys; and two types of basic shell construction: advanced skin stringer and composite honeycomb sandwich. This produced a total of six material construction variations for intermediate stage, pump-fed, storable liquid propellant tankage systems. The intermediate stage design is based on requirements typical of near-future three-stage booster systems capable of injecting payloads of at least 30,000 lb into a 300-naut-mile orbit, which established a study model with 330,000 lb of usable propellant. To provide the variations in loading, three payload planform areas were employed on the three-stage booster, which when coupled with two first-stage thrust levels, provided a total of six different loading configurations. Six variations in tankage geometries, within realistic constraints of the total vehicle, provided the means by which optimum tankage designs were identified for a particular loading configuration, alloy system, and type of construction. The most promising tankage designs resulting from the 216 configurations analyzed were evaluated for producibility and costs. Results indicate that optimum geometric relationships do exist, and that composite titanium honeycomb sandwich construction, titanium face sheets with aluminum core, are superior.

Introduction

IMPROVEMENT of booster system performance is a prime goal for advanced systems engineering. To effect increased payloads and velocities, while still employing current and near-future booster vehicles, advanced systems technology is required to delve deeply and specifically into system design refinements that will increase booster vehicle performance. Generally, booster system performance can be increased by using higher energy propellants or by increasing the propellant mass fraction through improved system design. The objective of the present parametric design analysis study was to identify those intermediate-stage advanced tankage designs for storable liquid-propellant, pump-fed, booster systems that will increase mass fraction; this is particularly desirable for upper stages of a booster vehicle system because of the larger performance gains that can be realized. The study results were used to identify an applied research tank design suitable for subscale fabrication and development.[1]

Increases in material strengths tend to reduce required material thickness and tank weight, if that thickness is a function of material allowable. Liquid propellant pump-fed tankage systems do not always have sufficient internal pressure to maintain stability of the structure throughout the loads regime. As a result, skin-stringer shell construction is commonly employed today. A sandwich-type construction, employing stabilizing lightweight core, that permits the use of thin-wall structures associated with high material allowances is being developed. This paper considers materials and construction tradeoffs for various tankage configurations on representative launch vehicle configurations.

The results question the desirability of pursuing the development of production processes for titanium and steel integral-skin-stringer tankage. The integral skin-stringer configuration required to provide an efficient structure is difficult to machine. The honeycomb sandwich concept, on the other hand, provides the required rigidity through the fabrition technique. As materials with higher strength-to-density ratios become available, the sandwich concept, which is predicated upon satisfactory fabrication techniques, should produce highly efficient structures, the demonstration of which is the objective of phase II of the subject contract.[2]

Study Model

The size selected for the intermediate-stage study model was established to derive maximum application to near-future booster systems and indicated that an orbital capability of at least 30,000 lb should be considered. As a result, the intermediate stage of a three-stage booster vehicle was defined to have a usable propellant capacity of 330,000 lb of N_2O_4/0.50 UDMH-0.50 N_2H_4, which delivered 35,000 lb into a 300-naut-mile orbit.

Figure 1 illustrates the intermediate-stage study model arrangement for the parametric study. The study model em-

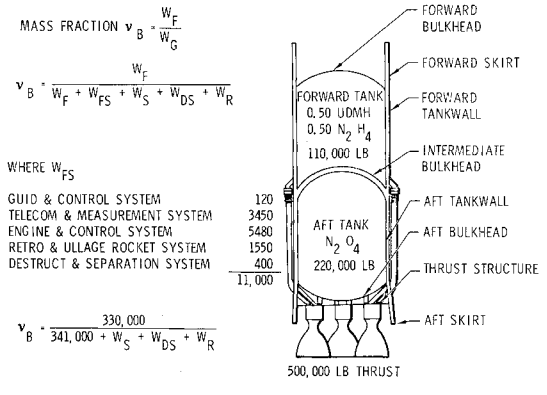

Fig. 1 Study model.

Presented at the AIAA Fifth Annual Structures and Materials Conference, Palm Springs, Calif., April 1–3, 1964 (no preprint number; published in bound volume of preprints of the meeting); revision received October 5, 1964. The analysis presented was performed as part of the Advanced Tankage Configuration Study sponsored by the Air Force Rocket Propulsion Laboratory, Research and Technology Division, Edwards, Calif., Air Force Systems Command, U. S. Air Force, under Contract AF 04(611)-8505. The author thanks R. L. Wiswell, Air Force Project Officer, and D. W. Carter, E. F. Blum, J. W. Holt, J. C. Mitchell, and G. W. Morgan of North American Aviation's Space and Information Systems Division for their contributions to this U. S. Air Force parametric booster tankage design analysis.

* Project Manager, Advanced Systems, Space and Information Systems Division. Member AIAA.

ploys four typical 125,000-lb thrust second-stage engines with a total thrust of 500,000 lb. The tankage major components are also identified. A common bulkhead is employed to maximize propellant mass fraction. Also shown is a conical thrust structure providing support for the four 125,000-lb thrust engines.

The objective of identifying tank designs leading to improved mass fractions was further simplified by fixing other systems associated with the intermediate stage not appreciably affected by changes in the tankage configuration. These are tabulated in Table 1. This includes the engine systems with their estimated weight and results in a total fixed systems weight (W_{FS}) of 11,000 lb.

The tankage design variation will affect the structural weight (W_S), dependent system weight (W_{DS}), and residual weight (W_R). The dependent systems' weights are those associated with propellant lines, electrical wiring, and pressurization systems. The residual weights are trapped propellant and residual gas weights. The propellant mass fraction is, therefore, defined by the equation

$$\nu_B = \frac{W_F}{W_F + W_{FS} + W_S + W_{DS} + W_R} = \frac{330{,}000}{341{,}000 + W_S + W_{DS} + W_R}$$

Thus the design analysis objective is the reduction of the structural weight (W_S), dependent systems weight (W_{DS}), and residual weight (W_R). Mass fractions in excess of 0.968 cannot be achieved with this study model, because the weight of the structure and residuals would have to be zero. The difference between 0.968 and the actual stage mass fraction is a function of tankage design.

Booster Vehicle

The general booster vehicle study parameters pertain to the total vehicle configuration of which the previously discussed study model is a part. Two three-stage base-point booster vehicle configurations provide the basis for the load and trajectory analysis and interstage interface requirements. These configurations are defined as capable of injecting at least 30,000 lb into a 300-naut-mile orbit. The vehicle mission requirements also provide a major portion of the ground rules upon which the parametric design analysis study is based.

To provide variation in over-all vehicle loads, three payload planform areas have been selected: 100, 660, and 1200 ft², representing Apollo, Dyna-Soar, and a lenticular-type payloads. To provide variation in first-stage acceleration, two first-stage booster systems were selected: a storable liquid and a clustered solid segmented propellant motor. The combination of first-stage thrust over weight ratios (T/W), and the three payload planform areas provide six different loading configurations to identify the influence of vehicle configurations upon the intermediate stage design.

Trajectory data for the two study vehicles are necessary to size the vehicles and derive typical loads and temperature criteria. Vertical boost for 12 sec was followed by a programed turn into a zero-lift trajectory (gravity turn) and termination of the gravity turn, and optimum steering to

Table 1 Fixed system weights

System	Weight, lb
Guidance and control system	120
Telemetering and measurement system	3,450
Engines and engine control system	5,480
Retro and ullage rocket system	1,550
Safety equipment and separation system	400
Total	11,000

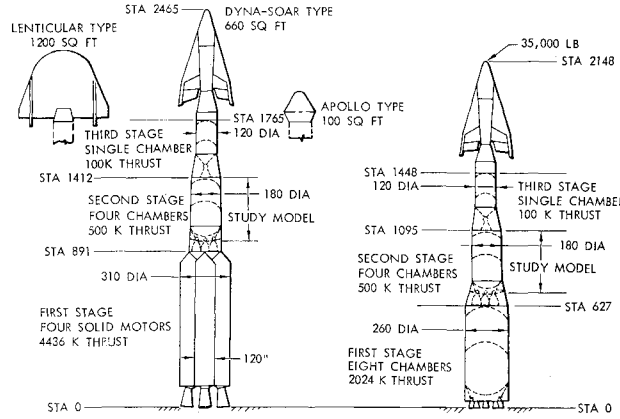

Fig. 2 Base-point booster vehicles.

100 naut miles was utilized until reaching the Hohmann transfer velocity for the desired 300-naut-mile orbit. Impulsive burning of the third stage was assumed for the orbital injection maneuver.

Base-Point Booster Vehicle Configurations

To identify pump-fed advanced tankage designs leading to an increase in mass fraction, vehicle base-point configurations (Fig. 2) were established defining the parametric boundaries.

First identified, because of the limited design variations of solid propellant systems, was the size of the solid-propellant first stage. This fixed the payload capability at approximately 35,000 lb, to which the size of the liquid-propellant first stage was matched. As a result, propellant weight distribution among the upper stages was not necessarily optimum for the given payload weight.

The primary difference imposed on the intermediate stage tank design by the two base-point systems was essentially one of acceleration, dynamic pressure loads, and aerodynamic heating.

An *all-storable liquid-propellant three-stage booster vehicle* with a 660-ft²-planform winged payload is illustrated in Fig. 2. It has a gross weight of 1,668,000 lb and a payload weight of 35,000 lb. Eight engines, each with a 253,000-lb thrust, are employed in the first stage, the usable propellant capacity of the first stage being 1,065,000 lb. The total first-stage thrust of 2,024,000 lb results in an initial T/W of approximately 1.2. The second stage, the subject and model of the parametric study, employs four 125,000-lb thrust engines. The propellant weight of this stage is fixed at 330,000 lb. To keep parametric analysis within manageable scope, study model applied loads for a given payload planform area were assumed constant. The third stage employs one 100,000-lb thrust engine. The usable propellant weight on this stage is 100,000 lb, which results in a begin-third-stage boost (T/W) of approximately 0.7.

The *solid-propellant first-stage base-point vehicle* is also illustrated schematically in Fig. 2. The upper stages (including payload) are identical to those of the all-liquid storable system. The first stage consists of a cluster of four 120-in.-diam solid-propellant motors to provide a total thrust of approximately 4,400,000 lb. The vehicle has a gross weight of 2,546,000 lb resulting in an initial T/W of approximately 1.75.

Figure 2 schematically illustrates three payload planforms used in this study. The range of planform areas was intentionally broadened for the payload weight of 35,000 lb to insure that lateral loading trends caused by payload configuration would be identified in the parametric design analysis. Drag effects of the payload variations on the study model are neglected, and the axial loading due to the payload configurations

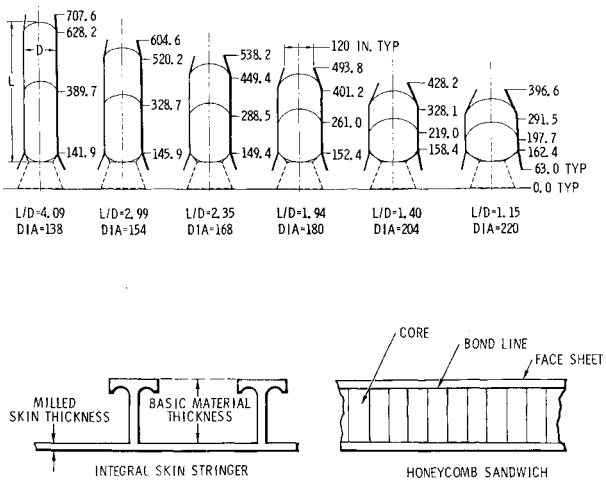

Fig. 3 Fineness ratio geometries and shell construction concept.

is assumed identical to keep the study within manageable scope.

Base-Point Booster Vehicle Loads

Structural loads for the two base-point configurations, each with three payload planform areas, were computed by the design analysis machine program predicated upon the aerodynamic coefficients of the vehicle configurations. To keep the study within manageable scope, rigid body dynamic and instantaneous controls were assumed. As a result, the study model has a total of six loading configurations employed as a primary parameter.

All basic loads used in the design analysis were obtained directly from the trajectory data and loads criteria, except for the maximum dynamic pressure condition, which is based upon the angle of attack. The synthetic wind profile employed was based upon the 99% wind velocity envelope and 99% wind shear for the windiest month at Cape Kennedy.

Five basic design loading conditions, based on the design criteria derived from past Space and Information Systems Division (S&ID) studies that were used in the design analysis, are: 1) prelaunch (free standing), 2) begin boost stage I, 3) maximum dynamic pressure (lateral loading), 4) end boost stage I, and 5) second-stage operation (maximum skin temperature) which includes begin boost, midboost, and end boost. The solid-propellant configuration imposed greater loads on the study model due to higher dynamic pressure as a result of the higher T/W ratio.

Tank Design

Tank Geometry and Principal Structural Components

The geometry (L/D) or fineness ratio and principal structural components are directly related, i.e., as L/D varies, so do the structural components. Six L/D ratios from 1.15 to 4.09, as illustrated in Fig. 3, were established for this study. The principal structural components are the interstage, forward bulkhead and tank wall, intermediate bulkhead, aft tank wall and aft bulkhead skirt, and thrust structure, as shown in Fig. 1.

The diameter of a given booster or tank is dictated to some degree by the minimum envelope required by the propulsion system, while sufficient space must also be provided in the interstage area to properly house the rocket engines and their control angle displacement. Therefore, the range of tank geometries (length-over-diameter ratios) are kept within practical limitations.

Tank fineness ratio (L/D) (Fig. 3) is defined as the length of the stage tankage from bulkhead crown to bulkhead crown divided by the diameter of the cylindrical tank. Care was taken to assure that the range of fineness ratios investigated for each configuration would be broad enough to indicate optimum tankage weights.

The design and shape of a bulkhead are dependent on several factors: the number of engines, propellant density, plumbing complexity, propellant utilization, etc. These are some governing factors in the shape of the intermediate or common bulkhead. Past studies at S&ID indicate that an elliptically shaped bulkhead with the concave face aft is a near-optimum arrangement for the intermediate bulkhead and was, therefore, established in the study model. The design and shape of the aft bulkhead is predicated not only upon the thrust level but also upon the number of engines and whether the thrust structure and aft bulkhead are integral. For the purposes of this study, four engines have been selected, decreasing the applicability of an integral aft bulkhead thrust structure.

In an optimum weight analysis, evaluation of any particular component requires investigation of its effect on the overall structural system. For instance, for a given propellant mass, variations in the geometry of the tankage length-to-diameter (L/D) will change the structural requirements. Also, variations in the aspect ratio of the bulkheads will affect length and weight of the interstage construction, whereas variations in the diameter for a fixed internal pressure will affect the discontinuity relationships at the bulkhead-to-cylinder joint. For example, a hemispherical dome may be optimum from a pressure-vessel standpoint, whereas the weight required for a longer interstage structure may not be optimum. In addition, the structural design evaluation includes the influence of various trajectories, the implementation of various fabrication techniques, and structural properties of the selected alloy systems.

Materials and Construction

The selection of materials for low-weight, maximum strength structure for large boosters leaves but a few probable candidates. Of the materials that have very high strength-to-weight ratio advantages, only three have suitable characteristics for fabrication of a structure of the advanced tankage complexity. This study considers these three materials for producibility: aluminum, stainless steel, and titanium.

The alloys of aluminum, steel, and titanium, which have obtained some usage in the aerospace industry, show the most promise for increasing mass fractions in the near future. Associated with the three structural alloy systems, two advanced tank wall construction techniques are identified: skin stringer and honeycomb sandwich (Fig. 3). The honeycomb core in all cases is aluminum. The aluminum skin-stringer construction for this study is an advance in the present state of the art and is used as a nominal base for comparison between other material-construction techniques. Minimum skin gage thickness limitations delineated for both types of construction, anticipating advancement of the state of the art, are: 0.006 in. for steel, 0.008 in. for titanium, and 0.010 in. for aluminum.

To keep the study within manageable limits, each tank design employed a single alloy for all the principal structural components, with the exception of the core material, which is aluminum. This study did not intermix different alloys for the various structural components, although it is possible that this could be employed to gain a further increase in mass fraction.

The principal material variables that require consideration are strength properties, thickness of the face skin, and orientation of nonisotropic skin material. Variables unique to honeycomb core are structural strength properties, thickness, and orientation of cells, whereas for the skin stringer, the orien-

tation and spacing of frames and stringers are of primary concern.

For this design analysis three structural alloys were selected: 2014-T6 aluminum, PH16-7 Mo steel, and 6Al-4V titanium. Material properties are presented in Table 2. The selection of these materials is based upon the following properties and characteristics: 1) compatibility with the propellants, N_2O_4 and 50/50 UDMH-hydrazine, 2) availability, 3) strength-density ratio, 4) elastic modulus-density ratio, 5) ductility, 6) toughness, 7) fabricability, and 8) weldability.

Based on theoretical structural analysis and experience in building aircraft and aerospace structure, two types of construction methods have been recognized as the optimum in structural efficiency: skin stringer and honeycomb sandwich (Fig. 3). The advanced skin-stringer construction is identified as the machined integrally stiffened panel, which, for the purpose of this study, is considered to be an advanced state-of-the-art capability. This method eliminates potential sealing problems that accompany mechanically attached stiffeners and permits stringers, attach points, and frame caps to be strategically located. Skin thicknesses can be varied to meet specific structural requirements. An alternate method of producing integral skin-stringer panels is extrusion; facilities exist for aluminum, but at present are restricted to comparatively narrow panel widths that increase the weld-joining requirements. The honeycomb structure is identified as an inner and an outer skin of one of the three materials under consideration bonded to an aluminum honeycomb core. The inner skins can be welded together to produce a continuous structure.

Propulsion Systems

The propulsion system parameters selected are those associated with a typical second-stage storable propellant system. Although the basic engine weight is designated as a fixed system, the pressurization and propellant feed systems are dependent systems, that is, contingent upon the stage configuration. The fixed system weights include weights such as engine weight and vector control weight that do not appreciably change with changes in configuration.

The dependent and residual system weights are, however, a function of tankage configuration. Rocket engine turbopump ullage pressure requirements as a function of fineness ratio, together with propellant and heat protection parameters, are presented in Fig. 4. To establish the residual weights, it was assumed that the propellant tanks would be emptied at thrust termination but the feed lines would remain filled. In all cases, the propellant tanks were assumed to contain pressurization gases at thrust termination. Hardware includes propellant lines, valves, line supports, sensory and pressurant receiver. The curve is an extrapolation of existing data which was not necessarily an optimum system weight. These weights, however, do reflect a consistent

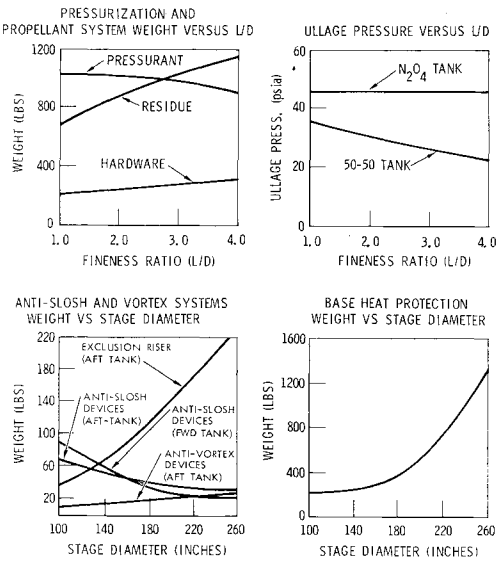

Fig. 4 Propulsion system parameters.

weight influence as the tank fineness ratio is varied. Antislosh and antivortex devices and heat protection requirements are also a function of tankage configuration. Weights for these devices have been estimated as functions of tank diameter (Fig. 4). In all cases, the material used for antivortex, antislosh devices, and heat shield was considered to be aluminum. Further analytical refinement is required if specific vehicle configuration is considered.

Structural Criteria

The expected maximum operating temperature of the interstage and tank-wall structure is required to compare the three alloy systems and the two types of construction. The temperature response of the structure is a function of the aerodynamic heating, based upon the trajectories of the base-point configurations presented earlier and the material-construction concept. The thermal and structural analysis includes variations in core and face sheet thickness and materials to indicate expected ranges in temperature response of the shell wall or interstage structure. The aerodynamic heating and structural temperature history for two points on the intermediate stage representing the tank-wall and interstage structure were used. Temperatures as high as 400° F on the interstage sandwich outer skin were identified.

One of the principal modes of failure of pressurized cylinders subjected to combined axial and bending loads is the phenomena of general instability, or shell buckling. Control of it, with corresponding improvements in vehicle mass fraction, develops directly from the mathematical model

Table 2 Material properties of aluminum, stainless steel, and titanium

Representative alloy	T, °F	Allowable stress, ksi: Compression at yield F_{cy}	Tension ultimate F_{tu}	Tension at yield F_{ty}	Modulus of elasticity 10^4 psi, E
2014-T6 aluminum	78	60	67	59	10.5
	300	49	58	50	10.1
	400	41	46	40	9.6
Steel PH16-7 Mo (RH 1075)	78	185	190	170	30.0
	300	178	181	148	28.9
	500	167	167	136	27.0
Titanium 6AL-4V (STA)	78	150	155	145	16.3
	300	120	136	119	15.5
	600	105	122	97	14.3

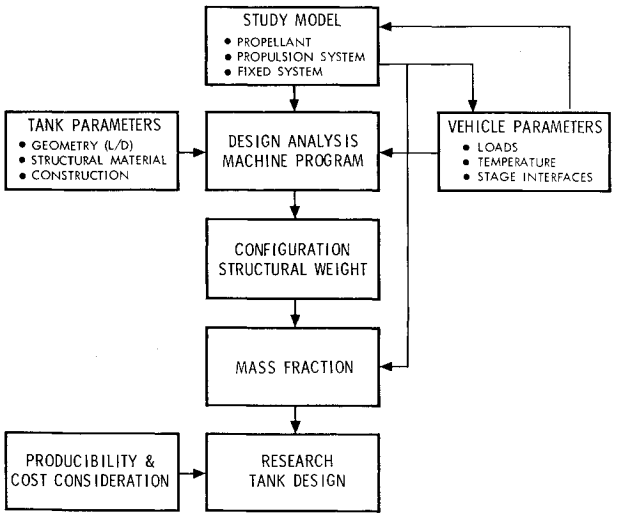

Fig. 5 Parametric design analysis.

from which the general instability conditions are determined. The reliability of the instability equation depends upon the accuracy of the assumed circumferential stress distribution of orthotropic cylindrical shells acting under combined bending and axial loads. Both the skin stringer and the honeycomb sandwich types of cylindrical structures exhibit orthotropic properties, which introduce rigidity properties different from those of isotropic structures. In addition to the shell instability and the rigidity coefficients of the orthotropic cylinders, the structural analysis will consider the effects of various vehicle design allowables on loading indices and weight ratios of the structural components. This study is central to an analysis of the contributing effects and trends of the thrust, bending and pressure loads, the capability of various materials and constructions to resist the imposed loads, and the relative structural efficiencies of the material-construction combinations.

The structural design criteria that are used for design purposes are defined as follows: limit load = actual applied load; ultimate load = 1.4 × limit load; yield load = 1.0 × limit load; proof pressure = 1.10 × maximum working pressure; and burst pressure = 1.25 × maximum working pressure. The maximum working pressure is the design pressure plus the maximum accumulation of regulation system tolerances. The minimum pressure that can be reasonably expected to occur in the event of pressurization-system failure is assumed equal to the propellant vapor pressure which is also a function of time and temperature. For loadings in which pressure effects are additive to externally applied loads, maximum working pressure and applied loads are both multiplied by the appropriate factor of safety. For loadings in which pressure effects are relieving, the minimum pressure is combined with the externally applied limit load.

Study Results

The parametric design analysis, incorporating the parameters and criteria established in the preceding section, was performed on the study model as illustrated in Fig. 5. A machine program was utilized in deriving the structural weight for each of the 216 configurations, which result from six tank geometries, six material construction concepts, and six design loading configurations. In deriving the stage mass fraction, the structural weight of each of the configurations incorporated the dependent systems and the residual weight as delineated in the study model (Fig. 1).

Structural Weight

Results are presented as a function of fineness ratio for each of the payload areas. Figure 6 (top) illustrates structural weight vs fineness ratio for the 100-ft² payload cases for both first-stage boosters; however, the study trend for the construction method was not consistent. Titanium integral-skin-stringer construction was optimum for low L/D for the solid first-stage system, whereas titanium honeycomb sandwich construction was optimum throughout for the liquid. The effect of increased temperature on the thin-gage facing sheets of the sandwich construction as a result of low load intensity appears to be the cause, i.e., low tank L/D's decreased the skin gage requirement and resulted in increased structural temperatures. The range in optimum tankage design weights for both systems varied from 5250 lb for Ti honeycomb sandwich to 8600 lb for Al honeycomb sandwich. Near-optimum fineness ratios were obtained for L/D's greater than three and appear to be insensitive for additional increases in fineness ratio.

With the 660-and 1200-ft² payloads, Ti honeycomb sandwich was optimum for both solid and liquid propellant systems. The 660-ft² designs varied from 6300 lb for Ti to 10200 lb for Al, with an optimum fineness ratio of approximately 2.5 (Fig. 6, middle); the fineness ratios were more sen-

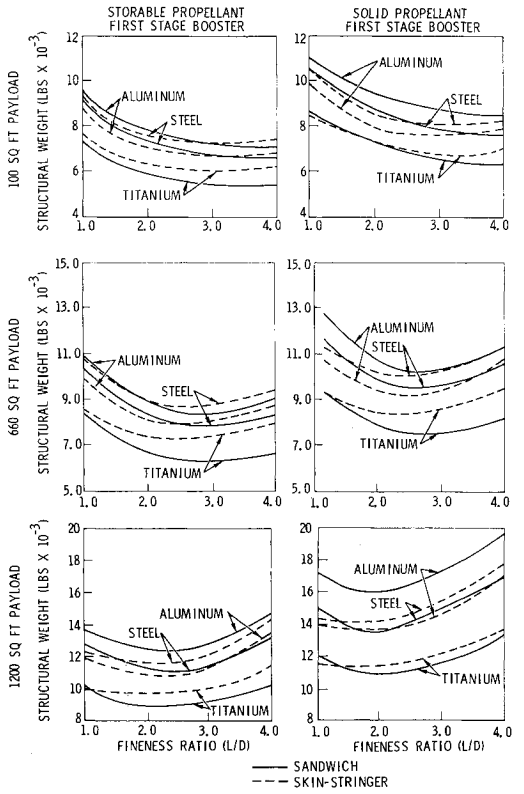

Fig. 6 Intermediate stage structural weight vs fineness ratio for 100-, 660-, and 1200-ft² payloads.

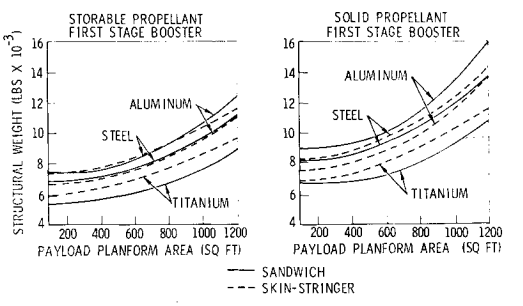

Fig. 7 Intermediate stage structural weight vs payload planform area, L/D = 2.35.

sitive to structural weight because of higher design load criteria imposed by the larger payload area. The 1200-ft² designs varied from 8850 lb for Ti to 15,950 lb for Al, with an optimum fineness ratio of approximately 2.0 (Fig. 6, bottom).

The structural weight for all configurations increases as the planform area increases with the titanium sandwich construction indicating minimum weight design as shown in Fig. 7 for an L/D of 2.35. In addition, the effect of the first-stage booster can be observed by noticing the relative positions of the various material construction concepts, i.e., higher T/W solid first stage requires more structure; furthermore, minimal slope in the small payload planform area indicates that design conditions other than bending are becoming dominant, i.e., load intensity is lower.

Stage Mass Fractions

Stage mass fractions were derived for the study configurations by incorporating the fixed system weight W_{FS} (Fig. 1) and associated dependent systems weight W_{DS} and residual weight W_R (Fig. 4) with stage structural weight W_S (Fig. 6). An optimum design configuration of titanium honeycomb sandwich was identified as providing the highest mass fraction. In addition, alternate configuration studies of the first and third stages were made and are similar to those derived for the intermediate stage. Performance gains for the advanced designs are delineated, predicated upon the state-of-the-art base-point design.

Mass fractions as high as 0.946 were obtained, which represent a maximum value for these configurations. However, this also represents the stage mass fraction incorporating fixed systems of 11,000 lb, which, of itself, makes mass fractions higher than 0.968 an impossibility when based on 330,000 lb of propellant. The stage mass fractions for all 216 configurations (based on the study model) were derived employing the results from the design analysis machine program. Figure 8 (top) illustrates stage mass fraction vs fineness ratio for the 100-ft² payload configuration. The optimum mass fractions vary from 0.946 for a Ti honeycomb

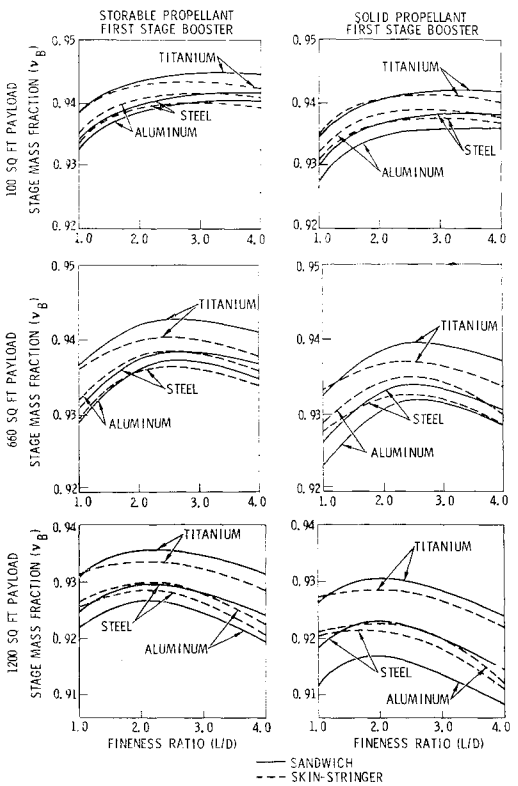

Fig. 8 Intermediate stage mass fraction vs fineness ratio for 100-, 660-, and 1200-ft² payloads.

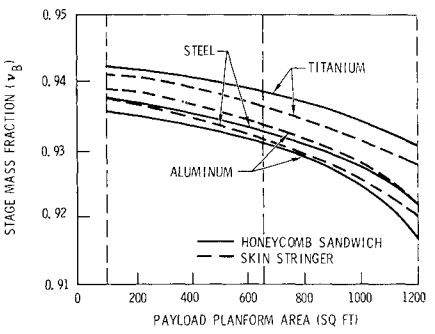

Fig. 9 Intermediate stage mass fraction vs payload planform area, solid-propellant first-stage booster, L/D = 2.35.

construction to as low as 0.936 for an Al honeycomb design. Figure 8 (middle) shows similar curves for a 660-ft² payload configuration: optimum mass fractions varied from 0.9426 for Ti honeycomb construction to 0.932 for an Al honeycomb sandwich design; and Fig. 8 (bottom) shows variations from 0.9358 for Ti honeycomb to as low as 0.917 for Al honeycomb for the 1200-ft²-payload configuration.

Cross-plots of stage mass fraction vs payload planform are for the three alloys and the two construction methods are given in Fig. 9. Because of the apparent advantages of the Ti honeycomb sandwich designs, where larger payload areas were involved, the solid-propellant first-stage booster which imposed the greatest loads was selected for comparison. From this study and predicated on state-of-the-art advances, the advanced tank design selected for development as an applied research tank design was based on a 660-ft² payload area employing a solid-propellant first-stage booster vehicle with a Ti honeycomb sandwich intermediate-stage tank design. This design showed an improved mass fraction from 0.914 for the original base-point configuration to 0.9395. The optimum L/D was identified as 2.6. Detailed analysis of the optimum titanium tank design confirmed the machine program results that established the basis for the development of an applied research tank design (Fig. 10).

Comparison of the intermediate stage mass fractions also was conducted by determining stage mass fractions for both the first-stage and third-stage storable systems, as illustrated in Fig. 2, with the 660-ft² payload (Fig. 11). Titanium construction provided the maximum mass fraction designs, here also exceeding 0.955 for the first stage, whereas the third stage obtained a mass fraction of 0.914.

Performance Improvement

Compared to the base-point configuration mass fractions (current state of the art), the various improved mass frac-

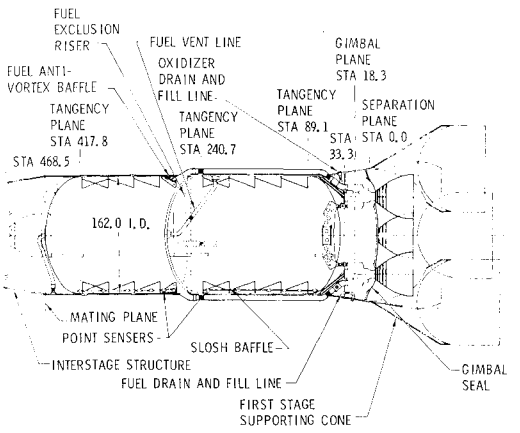

Fig. 10 Composite titanium honeycomb tank design.

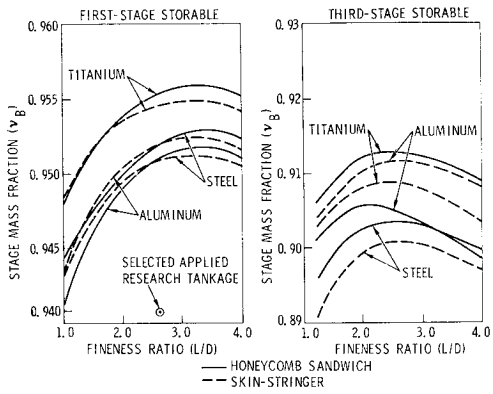

Fig. 11 Alternate configurations stage mass fraction vs fineness ratio, 660-ft² payload.

tions represent the following increases in payload. These comparisons do not consider the effect of the increased payload weights on the third and intermediate stages, which would tend to decrease these mass fractions. These comparisons are presented primarily to illustrate the improvement that can be derived by advanced tankage design. For the 660-ft² payload configuration, this effect is minimal.

The mass fraction improvement in the intermediate stage from 0.914 to 0.9395 increased orbital payload by 2300 lb. The improvement in the third stage from 0.880 to 0.913 increased payload by 4150 lb. Thus a payload improvement of 6680 lb over the 35,000-lb base-point configuration resulted. In comparison, the Al honeycomb sandwich second- and third-stage design combinations increased orbital payload by a total of 4250 lb.

The analysis showed that, for every pound of inert weight saved on the intermediate stage, the orbital payload can be increased by 0.24 lb. The third stage, of course, has a pound-for-pound relationship between inert weight and payload orbited.

Producibility and Cost Considerations

Producibility and cost comparison studies were made to uncover any major differences for the development of the advanced tankage design. These studies were based upon a 10-yr development of an intermediate stage associated with a solid first-stage booster and 660-ft² payload loading configuration with the near-optimum tank L/D of 2.35 employed as a base. These estimates are based upon advances in the state of the art and the size delineated.

The producibility evaluation is based upon tank configurations of the same geometry and advances in the state of the art for each material-construction. Advanced material-construction configurations are considered from a producibility and comparative standpoint considering the optimum or near-optimum cases for tank design. All honeycomb sandwich configurations are bonded to Al honeycomb core. The following evaluation is predicated on current estimates (1962) of future development required to implement the production of high-strength tankage structure of the size delineated in the study. Comparative producibility estimates among the various material-construction configurations are presented in Table 3. To derive a more meaningful estimate, the table differentiates between tooling and fabrication processes in the construction of the tank.

The cursory cost comparisons shown in Table 4 were based on the following ground rules:

1) Costs considered are only those associated with an intermediate stage of a three-stage vehicle, in particular, the intermediate stage associated with the solid first-stage booster and 660-ft² payload loading configuration.

2) The cost analysis is based on the fabrication of three tanks for the research and development program and the production of 100 units over a 10-yr period.

3) The Al skin-stringer tank is selected as the base because of the availability of background data from such sources as Ref. 3.

The percentage of complexity of each of the five configurations compared to the base-point advanced aluminum skin stringer is based upon estimates from engineering, testing, and production. These complexity factors are applied to the items of the base estimate to obtain the estimates for the other five configurations. To simplify the comparisons, items that are associated with the stage, other than those directly related to the tankage, were assumed to be the same for all configurations considered. All data assumed 100% reliability.

Research and development items selected to provide the most significant comparison in the three-unit research and development phase are engineering, tooling, structure, ground tests, and other costs. Associated other costs include engines, guidance and electronics, ground support equipment, manufacturing and launch facilities, and propellant. Production tankage costs are based on identical ground rules for research and development tankage costs and include engineering maintenance, tooling maintenance, structure, production, testing, and other production costs.

A summary of the results of the total program cost comparison at the 100-unit production run is presented in Table 4. The Ti honeycomb sandwich tankage design, which was identified as optimum, appears to be less costly than aluminum or steel honeycomb construction at the 100 production run, even though it was heavily handicapped during the cost comparison (Table 3). This is primarily due to material/unit weight cost. However, tankage cost differences are negligible when compared on a program-dollar vs pound-of payload-orbited basis.

Study Conclusions

1) Stage mass fractions for tankage design increase as payload areas are decreased; this results from the lateral loading (bending moment) imposed by the payload area. The magnitude of the loading intensity the intermediate stage must take is directly related to the payload area. These

Table 3 Comparative material-construction producibility estimates

Type of construction	Tooling requirements	Fabrication
Aluminum skin stringer	Nominal; highly developed state of the art	Nominal; standardized fabricating procedures
Aluminum honeycomb	+20%; more tools, handling fixtures and facilities required	+15%; requires extensive processing, lay-up and bond-curing procedures
Steel skin stringer	+7%; rigid and precision tooling required	+10%; easy to weld but more difficult to machine
Steel honeycomb	+23%; size availability of material requires extra tooling	+17%; requires more weld-joining to achieve required sizes, material difficult to etch for bonding
Titanium skin stringer	+10%; material only available in small sizes, more weld tools required	+15%; titanium difficult to fabricate
Titanium honeycomb	+32%; tooling requirements more stringent	+30%; exactness of bond components hard to achieve severe forming requirements

Table 4 Cost estimates for 100 unit production over 10 yr

Description	Aluminum skin stringer	Aluminum honeycomb	Steel skin stringer	Steel honeycomb	Titanium skin stringer	Titanium honeycomb
Research and development, 10^6						
Tank (3 units)	81.4	100.0	85.6	103.1	88.4	103.2
Other costs	140.7	140.7	140.7	140.7	140.7	140.7
Total	222.1	240.7	226.3	243.8	229.1	243.9
Production and operations, 10^6						
Tank (100 units)	57.2	74.9	71.2	71.9	63.9	69.3
Other costs	390.1	390.1	390.1	390.1	390.1	390.1
Total	447.3	465.0	461.3	462.0	454.0	459.4
Total program, 10^6	669.4	705.7	687.6	705.8	683.1	703.3
Payload cost in orbit, $/lb	180	196	194	189	187	185

greater loads result in the requirement for efficient stiffened shell structure.

2) As the payload areas increase, the stage mass fraction optimize at lower tankage fineness ratios (L/D), and become more sensitive to variations in fineness ratio. The structure required for the greater bending moments caused by the larger payload areas becomes a higher percentage of the inert stage weight. As a result, the stage mass fraction becomes more sensitive to differences in tankage configurations.

3) Stage mass fractions are less sensitive to tankage design variations for small payload area (drag shape) cases, when "other-system" considerations become more important. The structural weight required to carry the reduced bending moment is a smaller percentage of the inert stage weight. As a result, other-system considerations tend to reduce the benefits derived from optimizing the tankage design from a pure structural approach.

4) Titanium tankage designs for the intermediate stage produce the highest mass fraction of the three materials investigated.

5) Titanium honeycomb sandwich tankage designs produced the highest mass fraction for lifting body payload. The higher strength-to-density ratio of titanium alloy, coupled with the honeycomb sandwich construction, provided the most efficient structure to carry the higher bending moments. Optimum stage mass fractions for the intermediate stage identified vary between 0.945 and 0.915, contingent upon the load configuration and material construction. This range in mass fraction for the intermediate stage alone represents a difference of 2700 lb in payload orbited from the base-point design, neglecting incremental inertia load effects.

6) Design analysis of the third stage presented the same trends as the intermediate stage, identifying titanium honeycomb construction as optimum, but the advantages are not as pronounced as those indicated for the intermediate stage. The third stage, which is located closer to the payload, has established different bending moment to axial load relationships. Optimum mass fractions identified in the design analysis vary from 0.901 to 0.913, depending on loading configuration and material construction; this range represents a difference of approximately 1700 lb in payload orbited from the base-point design, neglecting incremental inertia load effects.

7) Design analysis for a storable-liquid-propellant first stage indicated results similar to the intermediate stage, identifying Ti honeycomb as the optimum material-construction. The size and bending moment of the first stage were such that the advantage of the construction and higher strength-to-density ratio of Ti were realized. An optimum mass fraction of 0.9557 was obtained.

8) Predicated on the solid-propellant first-stage loading configuration, mass fraction improvements in the second and third stages utilizing titanium honeycomb construction can materially increase orbital payload. The mass fraction improvement, 0.914 to 0.9395, in the second stage increased the orbital payload to 2300 lb over the base-point configuration. The mass fraction increase, 0.88 to 0.913, in the third stage increased the orbital payload 4150 lb, for a combined orbital payload gain of 6680 lb over the base-point of 35,000 lb; the comparable gain for Al was 4250 lb.

9) Tankage costs of the six advanced material constructions, when compared on program dollars-per-pound-orbited, are approximately equal. Although the Ti honeycomb sandwich construction appears to be the most difficult to produce for the selected cases and results in the greatest expense per unit, the higher mass fractions derived allowed greater payloads to be orbited. This tended to equalize the cost on the basis of dollars-per-pound-payload-orbited. The advanced aluminum skin stringer was employed as a reference in comparing producibility cost conclusions.

References

[1] Morita, W. H., "Advanced tankage configuration study," Phase I Final Rept. (February 1963).

[2] Morita, W. H., "Titanium tankage development," Phase II Final Rept. (November 1964).

[3] "USAF cost optimized booster system studies," North American Aviation, Space and Information Systems Div. SID 61-341 (September 1961).